Mechanism of ion permeation through a model channel: Roles of energetic and entropic contributions

ARTICLE *in* THE JOURNAL OF CHEMICAL PHYSICS · OCTOBER 2013

Impact Factor: 2.95 · DOI: 10.1063/1.4827088 · Source: PubMed

3 AUTHORS, INCLUDING:

Takashi Sumikama

University of Fukui

10 PUBLICATIONS **42** CITATIONS

SEE PROFILE

Shinji Saito

Institute for Molecular Science

74 PUBLICATIONS **3,348** CITATIONS

SEE PROFILE

Mechanism of ion permeation through a model channel: Roles of energetic and entropic contributions

Takashi Sumikama,[1,a)] Shinji Saito,[2,b)] and Iwao Ohmine[2,c)]
[1]*Department of Molecular Physiology and Biophysics, Faculty of Medical Sciences, University of Fukui, Eiheiji-cho, Yoshida-gun, Fukui 910-1193, Japan*
[2]*Institute for Molecular Science, Myodaiji, Okazaki, Aichi 444-8585, Japan and The Graduate University for Advanced Studies, Myodaiji, Okazaki, Aichi 444-8585, Japan*

(Received 23 July 2013; accepted 11 October 2013; published online 31 October 2013)

Mechanism of ion permeation through an anion-doped carbon nanotube (ANT), a model of ion channel, is investigated. Using this model system, many trajectory calculations are performed to obtain the potential energy profile, in addition to the free energy profile, that enables to separate the energy and the entropic contributions, along the ion permeation. It is found that the mechanism of the transport is governed by the interplay between the energetic and the entropic forces. The rate of the ion permeation can be controlled by changing the balance between these contributions with altering, for example, the charge and/or the length of ANT, which increases the rate of the ion permeation by nearly two orders of magnitude. The dominant free energy barrier at the entrance of ANT is found to be caused by the entropy bottleneck due to the narrow phase space for the exchange of a water molecule and an incoming ion. © *2013 AIP Publishing LLC*. [http://dx.doi.org/10.1063/1.4827088]

I. INTRODUCTION

Mechanisms of transport and separation of the materials through nanopores have been intensively studied.[1–10] Carbon nanotube (CNT) and zeolite are examples of nanopores in material science which transport polymer, water, ions, and proton and are applied to molecular sensor and gene delivery.[11–33] It has been found that the flows of gaseous and water molecules through CNT are significantly, one to three orders of magnitude, faster than simplified theoretical predictions.[1–4] There are also intensive investigations on the water and ion permeation through biological nanopores, such as the aquaporins and the K^+ channels.[34,35] The molecular mechanisms of the ion permeation through biological channels are being well explored theoretically;[36–51] for example, by analyzing the free energy surface, Bernèche and Roux[41] showed how the ion motions are strongly correlated in the permeation process. Jensen *et al.*[47] recently performed the MD simulation of ion permeation through the Kv1.2 channel and showed that the ion permeation proceeds in the knock-on manner.

We have employed a simple model channel system,[52–59] an anion-doped CNT (ANT) in order to explore the precise molecular mechanism of the ion permeation by performing extensive trajectory calculations. In our previous study, we analyzed the mechanism of K^+ ion permeation through ANT.[59] It was found that the entering ion surrounded by its hydration water molecules in the bulk is mostly blocked by the repulsion from a water molecule locating at the entrance. The distinct free energy barrier was found at the entrance of the channel and only about 10% of K^+ ions reaching the entrance can enter the channel.

In the present work, we extend our study on the mechanism of the ion permeation through ANT by separating the potential energy contribution and the entropic contribution to the free energy surface. A great number of trajectory calculations were needed to obtain the energy profile, since the energy is a scalar quantity of a very slow convergence. This separation allows us to get insight into the precise molecular mechanism of the ion permeation; two kinds of the forces, namely, the energetic force and the entropic force, interplay in the permeation process by alternately acting on the ions. It is found that slight modifications of the charge and/or length of ANT change the balance of these contributions, which increases the rate of the ion permeation by about 80-fold at most among ANTs used in this study.

II. METHODS

The system consists of 24 K^+ ions, 1106 water molecules, eleven (6,6) armchair-type CNTs, and one (6,6) armchair-type ANT. The negative charges are helically arranged on ANT, the detailed configuration of negative charges on ANT is given in the previous paper.[59] Three kinds of negative charge on ANT are examined; total amounts of charge are −5.0e, −5.4e, or −6.0e.

The TIP3P model potential and default parameters of AMBER were used for water molecules[60] and K^+ ions,[61] respectively. AMBER94 sp^2 carbon was used for carbon atoms of CNTs and ANT.[61] The equilibrium bond length between carbon atoms was shortened from 1.4 to 1.2 Å to mimic the length, 12 Å, of the selectivity filter of the K^+ channel. The diameter of ANT was 7 Å.

MD simulations were performed at constant volume and constant temperature at 300 K with Berendsen's thermostat.[62] The intramolecular coordinates in water molecule were

a)Electronic mail: sumi@u-fukui.ac.jp
b)Electronic mail: shinji@ims.ac.jp
c)Electronic mail: ohmine@ims.ac.jp

constrained with the SHAKE algorithm,[63] and the time step for numerical integration was 2 fs. Long range interactions were calculated by the particle mesh Ewald method with an 11 Å real space cutoff.[64] The periodic boundary condition with the size of $31.306 \times 36.098 \times 43.010 \text{Å}^3$ was imposed.

In the simulations, passive transport of ions was realized by applying an electric field of 24 mV/Å along z axis, channel axis, in the region of ANT and CNTs ($5 < z < 21$ Å; see Ref. 59). This was to mimic the voltage-clamp measurement.[65] Total electric potential was 384 mV, which is lower than the upper limit of electrophysiological experiment.[66] The translation of ANT caused by the electric field was constrained by the harmonic potential with the force constant of 0.1 kcal/mol/Å^2. We generated 120 different initial configurations in which all K^+ ions were initially allocated in the bulk region. Each trajectory was calculated for 25 ns. Initial 500 ps were discarded and the data in the remaining 24.5 ns were used for the analysis. The trajectory was saved at every 10 fs.

The free energy profile of an ion along z axis is calculated by using the following equation:

$$\Delta F(z) = -k_B T \ln(P(z)/P(z_{\text{exit}})), \tag{1}$$

where k_B and T are Boltzmann constant and temperature, respectively. The free energy is defined as the difference of that at the exit, $z_{\text{exit}} = 5$ Å. The $P(z)$ is the existing probability that the ion is found at z,

$$P(z) = \int_0^{\text{box}_z} \int_0^{2\pi} \int_0^{3.5\,\text{Å}} \delta(z - z') e^{-H/k_B T} r\, dr\, d\theta\, dz', \tag{2}$$

where r, θ, box_z, and H are the radial coordinate which is perpendicular to z axis, the azimuthal angle, the cell size of the system along z axis, 43.010 Å, and the Hamiltonian of the system, respectively.

The energy profile along z axis was calculated by using the following equation:

$$\Delta\langle E(z)\rangle = \int_0^{\text{box}_z} \int_0^{2\pi} \int_0^{3.5\,\text{Å}} \delta(z - z') E e^{-H/k_B T} r\, dr\, d\theta\, dz' - \langle E(z_{\text{exit}})\rangle, \tag{3}$$

where E is the total potential energy of the system, not the interaction between an ion at a certain z and the system, and the brackets indicate an ensemble average.[67] The brackets of the above equation are omitted hereafter for simplicity. The total potential energy is defined as $E = E_{\text{ion-ANT}} + E_{\text{water-ANT}} + E_{\text{ion-ion}} + E_{\text{ion-water}} + E_{\text{water-water}} + E_{\text{ion-field}} + E_{\text{water-field}}$, where subscripts specify the components of the interaction energies; for example, $E_{\text{ion-water}}$ is the interaction between all ions and all water molecules. The interaction between ions and the electric field, $E_{\text{ion-field}}$, is expressed as

$$E_{\text{ion-field}} = \sum_{i=1}^{N_{\text{ion}}} E_{\text{field}}(z_i), \tag{4}$$

where N_{ion} is the number of ions in the system and $E_{\text{field}}(z_i)$ is the interaction with ith ion and the electric field shown in Fig. 1(b) in Ref. 59 (note the definition of z is shifted by 5 Å here). The energy profile, $\Delta E(z)$, was smoothed by the linear combination of 100 sine functions of its expansion,[68]

$$\tilde{E}(z) = \sum_{m=1}^{100} \sin\left(m\pi \frac{z}{\text{box}_z}\right). \tag{5}$$

The entropy ($-T\Delta S(z)$) profile along z axis was evaluated by subtracting the energy from the free energy; $-T\Delta S(z) = \Delta F(z) - \Delta E(z)$.

The adequacy of the sampling and convergence of the energy profile are confirmed by dividing the production trajectories into two equal blocks and comparing the energy profiles from each block. The difference between them is within 0.5 kcal/mol in general (at most 1 kcal/mol near the entrance, where the free energy is its highest), meaning the profile is well converged. The difference between those of the free energy profiles is less than 0.1 kcal/mol.

III. ION PERMEATION MECHANISM THROUGH ANT

Figure 1 shows the free energy (ΔF) profile, and its energy (ΔE) and entropic ($-T\Delta S$) contributions. In this figure (also in Figs. 3, 5, and 6), ions flow from right to left; from large z to small z (see movies S1 and S2 in the supplementary material).[69] In our previous study,[59] the analyses of a multidimensional free energy surface showed that the ions inside ANT move together almost without changing their mutual distance (the change is less than 0.6 Å, found in Fig. 3 of Ref. 59); the motions of ions in ANT are mutually strongly correlated. For example, the free energy barriers seen inside ANT ($z = 9.3$ and 14.0 Å) reflect that at the entrance ($z = 18.8$ Å). Accordingly, one-dimensional coordinate employed in the present work correctly captures the permeation dynamics through ANT, and thus we evaluated the energy and entropy profiles along this one-dimensional coordinate.

In this system, the free energy minima exist when two ions are inside ANT ($z = 10.8$ and 15.3 Å). We call this two-ion state S_2 hereafter. We can see in Fig. 1(b) that the configuration of ions in S_2 coincides with that at the minima of the entropic contribution ($-T\Delta S$). The configuration of ion at the minimum of $z = 10.8$ Å is, as mentioned above, almost equivalent to that at 15.3 Å. The configurations with three ions in ANT (will be called S_3 hereafter, the detail of this configuration is described later) correspond to the energetic minima, and are the metastable points in the free energy. Two ions and three water molecules are confined in ANT in the S_2 state, whereas three ions and four water molecules are confined in the S_3 state. The S_2 state thus has the more spatial (configurational) freedom for one ion and one water molecule and gains more entropic stabilization, in comparison with the S_3 state.

The free energy yields a nearly flat profile for the large z value just before the entrance at $z \sim 22$ Å, that is, ions can easily approach the entrance, as mentioned in the previous paper.[59] This is due to the cancelation between the energetic change and the entropic change, as seen in Fig. 1(b).

The ion then feels the large free energy barrier (2.2 kcal/mol) at the entrance at $z = 20.2$ Å, and most of the ions approached the entrance of ANT are thus repelled to the bulk (to the larger z). This free energy barrier at the entrance mainly arises from two entropic contributions. The

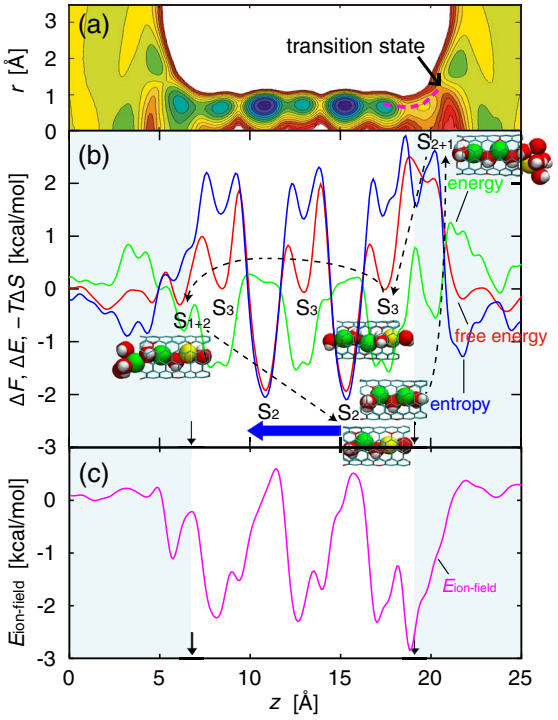

FIG. 1. Free energy (ΔF), energy (ΔE), and entropy ($-T\Delta S$) for the ion permeation through ANT with the charge of $-5.0e$ and the length of 12 Å. (a) The two-dimensional plot of the free energy along z, the channel axis, and r, the radial distance from z. Each color corresponds to an energy interval of 0.5 kcal/mol; reddish colors for higher free energies and bluish colors for lower free energies. The transition state at the entrance is indicated and the minimum free energy path from this transition state to S_3 is indicated by a dashed magenta line. (b) Free energy (ΔF), energy (ΔE), and entropy ($-T\Delta S$) along z are plotted in red, green, and blue lines, respectively. The bulk water region, i.e., the outside of ANT ($z > 19.0$ Å, $z < 7.0$ Å) is indicated with sky blue. The coordinates of the entrance and exit are indicated by small black arrows. Ions flow from large z to small z, as is indicated by a large blue arrow. Note that the z coordinate is shifted by 5 Å from that in Ref. 59. The overall process of the ion permeation is expressed as $S_2 \rightarrow S_{2+1} \rightarrow S_3 \rightarrow S_{1+2} \rightarrow S_2$. The broken arrows indicate the time course of the ion permeation. The snapshots for each state, where an entering ion is presented by yellow ball, are shown. (c) $E_{\text{ion-field}}$, the ion-field interaction, is plotted as a function of z. Note that $E_{\text{ion-field}}$ is a summation of the interaction of each ion with the electric potential shown in Fig. 1(b) of Ref. 59, thus it gives a nearly periodic saw-toothed shape in ANT. The slopes of $E_{\text{ion-field}}$ to the downstream are vestige of the interaction of each ion with the electric field, which generates the directionality of ion transport toward the downstream.

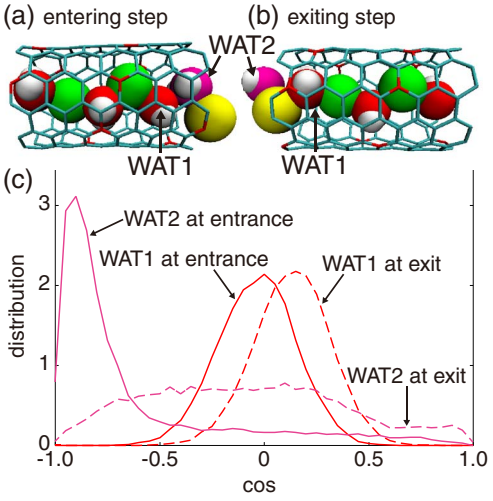

FIG. 2. Snapshots of WAT1 and WAT2 for the ion permeation through ANT with the charge of $-5.0e$ and the length of 12 Å at (a) the moment of ion entering and (b) the moment of ion exiting. Ions are transported from right to left. Green balls are ions in ANT, and red and white balls represent water. WAT2 is colored in magenta. Yellow ball is an ion entering or exiting. The definition of WAT1 and WAT2 are given in the text, as seen in (a), when an ion is entering. WAT1 and WAT2 are defined as seen in (b) when an ion (yellow) is exiting. When the ion permeation occurs, the entering ion exchanges its position with WAT2 to make the direct coordination to WAT1 at the entrance, while WAT2 exchanges its position with the exiting ion to make the direct coordination to WAT1 at the exit. (c) The orientational distributions of WAT1 (red) and WAT2 (magenta). The distributions for ion entering are shown in solid lines, and those for ion exiting are in dashed. The definition of θ is the angle between the dipole moment of the water molecule and the axis of channel, z.

first contribution to the entropic barrier arises from the restriction of the ion motion in the radial direction in ANT (Fig. 1(a)), which leads to the decrease in configurational entropy. This contribution is, however, estimated to be only 1.3 kcal/mol,[70] much smaller than the total entropic barrier height. The second contribution, that is, the main one, to the entropic barrier is found to arise from the orientational constraint of a water molecule locating at the entrance. We define here two kinds of water molecules WAT1 and WAT2: WAT1 is the water molecule directly coordinated to the ion located in the most upper stream inside ANT and WAT2 is the water molecule coordinating to this WAT1 (Fig. 2(a)). Since the ions and water molecules alternately permeate through ANT in a single file manner, the incoming ion must exchange the position with WAT2 in order to directly coordinate to WAT1. Just before this replacement between the ion and WAT2, WAT2 is sandwiched between WAT1 and the ion, and the orientation of WAT2 is strongly restricted, as indicated in Fig. 2(c) (movie S1 in the supplementary material).[69] This configuration of the ions shown in Fig. 2(a) is called S_{2+1}. At the same time, the orientations of other water molecules remain almost the same, not depending on the incoming or the outgoing ion position. As a result, the large entropic barrier exists at the entrance.

The highest saddle of free energy seemingly exists at $z = 18.8$ Å in the one-dimensional plot (Fig. 1(b)), while the highest locates at $z = 20.4$ Å and $r = 1.2$ Å in the two-dimensional free energy contour (Fig. 1(a)).[71] The transition path sampling analysis shows that this sandwiched WAT2 conformation of the S_{2+1} state, where the incoming ion locates between $z = 19.7$ Å and 20.2 Å, is the transition state, yielding near 50% probability of the ion permeation.[72]

After surmounting this entropic barrier (S_{2+1}; transition state), the system passes through a metastable free energy minimum, S_3, at $z = 17.6$ Å (the other ions are at $z = 8.4$ and 13.0 Å), where the energy itself yields the minimum. The overall energy decreases, except the energy peak at $z = 19.2$ Å, from $z = 20.4$ Å to 17.6 Å due to the field effect (see Fig. 1(c)). The ion translocation from the transition state, S_{2+1}, to S_3 at $z = 17.6$ Å is very fast (<10 ps; see below), so that the surrounding water molecules cannot be fully relaxed and the ion-water interaction, $E_{\text{ion-water}}$, is highly hindered (not shown in figures) in the process, resulting in the energy peak at $z = 19.2$ Å in Fig. 1(b). The stabilization of

$E_{\text{ion-ANT}} + E_{\text{water-water}}$ with the decrease of z is almost cancelled with the destabilization of $E_{\text{ion-water}} + E_{\text{water-ANT}}$, the change of $E_{\text{water-field}}$ is very small, and thus the energy minimum at S_3 is determined by the stabilization of $E_{\text{ion-field}}$. A profile of $E_{\text{ion-field}}$ along z has a saw-toothed shape with slopes toward the downstream (the smaller z) of ANT (in Fig. 1(c)). This saw-toothed energy slope produces the "energetic force" for the directional ion flux in the one-dimensional representation of correlated ion motions presently used.

Once briefly trapped in this S_3 state, the ions further translocate to the free energy metastable state (ions are z = 6.2, 11.1, and 15.4 Å; called S_{1+2}), by passing over a small free energy barrier by thermal fluctuation. In this S_{1+2} state, the left most ion is already outside of the exit of ANT and barely attached to ANT with small energy stabilization. This ion at the exit is easily hydrated to a bulk by crossing a small energy barrier originated from the ion-ANT attraction.

Figure 1(b) shows that there is no entropic barrier at the exit in contrast to the large entropic barrier at the entrance, because WAT2 at the exit ($z = 4.4$ Å) is immersed in the bulk and its orientation is much less constrained than WAT2 at the entrance, $z = 19.2$ Å (Fig. 2(c)). Here, see Fig. 2(b) for the definition of WAT1 and WAT2. Accordingly, its much broader orientational distribution results in the larger entropic stability than WAT2 at the entrance. Hence, the overall process of the ion permeation can be expressed as $S_2 \rightarrow S_{2+1} \rightarrow S_3 \rightarrow S_{1+2} \rightarrow S_2$, where the rate-determining step is $S_2 \rightarrow S_{2+1}$ (movie S2 in the supplementary material).[69] These steps are repeated as ions are transported through ANT.

In order to see how the energy and the entropy act on the ion flow in more detail, we analyzed the time dependent function $A(z; \Delta t)$ defined by

$$A(z; \Delta t) = -k_B T \ln(P(z; \Delta t)/P(z_{\text{exit}}; 0)), \tag{6}$$

where $P(z; \Delta t)$ is the distribution of ions being at the position z accumulated for Δt (Fig. 3). We set here that the system is at the transition state of the ion-WAT2 exchange, S_{2+1}, at $\Delta t = 0$. The $A(z; \Delta t)$ converges to the free energy at $\Delta t = \infty$. The derivative of $A(z; \Delta t)$ with respect to z is the "effective" force acting on the ions, which arises from both energy and entropic contributions, at Δt. In the transition state at $\Delta t = 0$ ps, three ions are locating at the purple points. At $\Delta t = 5$ ps (blue), S_3 starts to emerge and then becomes distinct at $\Delta t = 10$ ps (green). We can see that $A(z; 10\text{ ps})$ curve almost coincides with the energy profile (dashed green line). This shows that the dynamics from the transition state to S_3, up to Δt = 10 ps, is mostly controlled by the energetic force. After Δt = 60 ps, the S_{1+2} state emerges (orange). The $A(z; \Delta t)$ curve then becomes almost identical to the free energy profile (dashed red) after Δt = 300 ps (red) and the S_2 state is restored; the dynamics of ions from S_3 to S_2 is mostly governed by the entropic force, which becomes dominant for ion and water molecule to gain more degrees of freedom in the bulk than inside ANT.

Figure 4 plots Boltzmann's H-function defined by

$$H(\Delta t) = \int dz P(z; \Delta t) \ln \frac{P(z; \Delta t)}{P_{\text{eq}}(z)}, \tag{7}$$

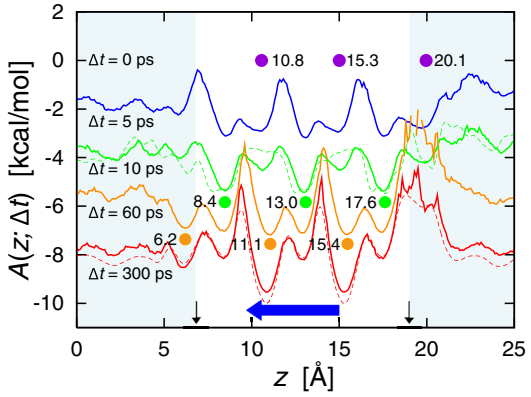

FIG. 3. Time dependence of the function, $A(z; \Delta t)$, after the exchange of WAT2 and the incoming ion, for the ion permeation through ANT with the charge of −5.0e and the length of 12 Å. The meaning of arrows and coloring are the same as in Fig. 1(b). The functions $A(z; \Delta t)$ at $\Delta t = 5$, 10, 60, and 300 ps are shown in blue, green, orange, and red, respectively. They are shifted by −2, −4, −6, and −8 kcal/mol, respectively. The energy and free energy profiles shown in Fig. 1(b) are also indicated in dashed green and dashed red, respectively. The positions of ions at $\Delta t = 0$, 10, and 60 ps are shown by the points in purple, green, and orange, respectively. The numbers beside the points are the z values of the ions. The energy profile (dashed green) resembles $A(z; 10\text{ ps})$ (green), meaning the motions of ions are controlled by the energy in short time. On the other hand, $A(z; 300\text{ ps})$ (red) is similar to the free energy profile (dashed red), meaning the dynamics of ions is governed by the free energy in long time.

where $P_{\text{eq}}(z)$ is the equilibrium distribution of the ions and the definition of time origin is the same as that in Fig. 3.[73] Note that the H-function corresponds to the entropy with negative sign. We can see in Fig. 4 that the H-function first yields a rapid decay caused by the thermal fluctuation at the transition state ($\Delta t < 5$ ps), and then reaches a plateau from 5 ps to 15 ps. The plateau means the "information" on the ion positions is not lost, that is, the entropy stays constant. This time duration (5-15 ps) when the plateau appears corresponds to the emergence of S_3 and thus the dynamics of the system

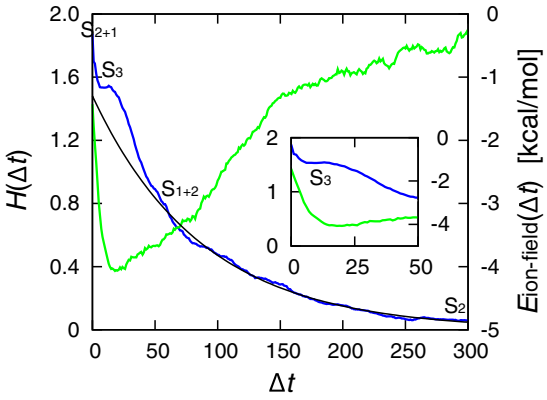

FIG. 4. Boltzmann's H-function and $E_{\text{ion-field}}$ for the ion permeation through ANT with the charge of −5.0e and the length of 12 Å. Boltzmann's H-function and $E_{\text{ion-field}}$ are indicated in blue and green, respectively. The inset shows the short time behavior of them. The plateau region, from $\Delta t = 5$ ps to $\Delta t = 15$ ps, indicates the entropy does not decrease, so the motion of ions are controlled by only the energy. The long time behavior of the H-function is well fitted by an exponential function shown in black, meaning the relaxation from S_3 to S_2 is a random process. The $E_{\text{ion-field}}$ is restored to the value of the upper stream when the system returns to S_2, thus the energy profile seen in Fig. 1(b) is flat.

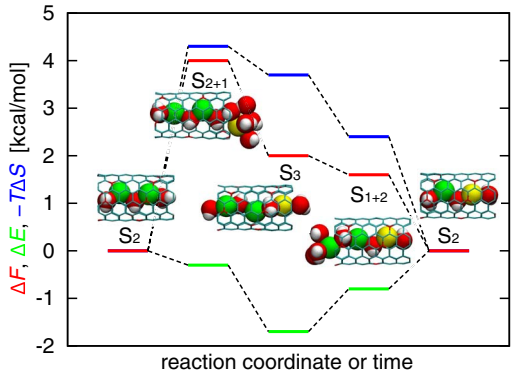

FIG. 5. The summarized diagram of ion permeation through ANT with the charge of −5.0e and the length of 12 Å. The red, green, and blue lines indicate the levels of the free energy, energy, and the entropy terms, respectively. The origin of energy levels is defined as that in S_2. The snapshots of each state are shown. Note that the levels of the energy and the entropy term resemble $E_{\text{ion-field}}$ and Boltzmann's H-function in Fig. 4.

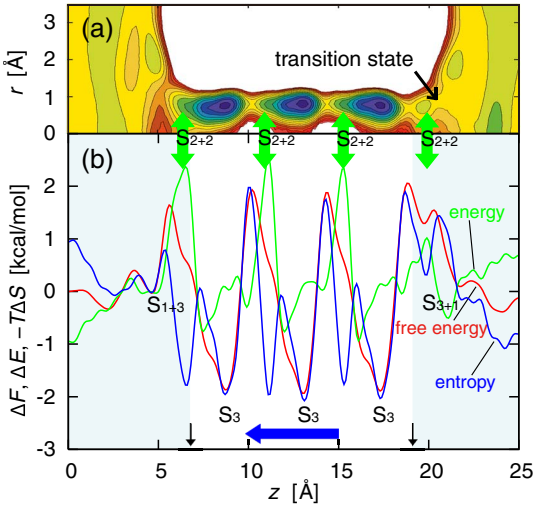

FIG. 6. Free energy (ΔF), energy (ΔE), and entropy ($-T\Delta S$) profiles for ion permeation through $ANT^{-6.0}$. The length of ANT is 12 Å. (a) The two-dimensional plot of the free energy along z and r. The method of coloring is the same as in Fig. 1(a). (b) Free energy, energy, and entropy along z are indicated in red, green, and blue lines, respectively. The meaning of arrows and coloring are the same as in Fig. 1(b) except the green arrows, which indicate the position of ions at S_{2+2}. The overall process of the ion permeation is expressed as $S_3 \rightarrow S_{3+1} \rightarrow S_{2+2} \rightarrow S_{1+3} \rightarrow S_3$.

from the transition state to S_3 state is mostly controlled by the energy. Then, the H-function starts to decay, so as the "information" on the ion positions lost and the entropy begins to govern the motions of ions. The H-function after $\Delta t = 50$ ps is well fitted by an exponential function which shows the process of the transition from S_3 to S_2 is expressed as Markovian (i.e., a random process).

The time change of the ion-field interaction, $E_{\text{ion-field}}$, is also plotted in Fig. 4 with a green curve. In the short time ($\Delta t < 15$ ps), the ions are driven for $S_{2+1} \rightarrow S_3$ by the energetic force arisen from the rapidly decreasing $E_{\text{ion-field}}$. The scheme of ion permeation through ANT is summarized in Fig. 5.

IV. MECHANISM OF ION PERMEATION THROUGH ANT WITH CHARGE OF −6.0E

So far, we have discussed the detailed mechanism of ion permeation through ANT with the charge of −5.0e. We also examined the mechanisms through ANT with different charges. Figure 6(b) shows the free energy, energy, and entropy ($-T\Delta S$) profiles for ion permeation through ANT with the charge of −6.0e. In order to distinguish the charge on ANT, the superscript is used hereafter. The shape and height of the free energy, energy, and entropic profiles of $ANT^{-6.0}$ largely change from those of $ANT^{-5.0}$ shown in Fig. 1, since $ANT^{-6.0}$ contains one more K^+ in its inside than $ANT^{-5.0}$ because of the stronger ion-ANT attraction. The free energy minima in $ANT^{-6.0}$ correspond to the three-ion state (S_3) with the ions locating at $z = 8.7$, 13.0, and 17.3 Å. Although the peaks positions of the free energy profile in $ANT^{-6.0}$ coincide with those of the entropy profile as in the case of $ANT^{-5.0}$ (Fig. 1(b)), the overall profile of the free energy in $ANT^{-6.0}$ is significantly modified from that of the entropic contribution because of the existence of the large energetic barriers (at the positions of green arrows in Fig. 6). It is noticed that the entropic peak at the entrance in $ANT^{-6.0}$ is significantly lower (by 1.1 kcal/mol) than that in $ANT^{-5.0}$ (Fig. 1(b)). This is because WAT2 is outside of $ANT^{-6.0}$ and not sandwiched between WAT1 and the incoming ion. The incoming ion can thus easily coordinate to WAT1, unlike in $ANT^{-5.0}$.[59] As an ion (the fourth ion) coordinates to WAT1, the system feels the energy dip of the S_{3+1} state with four ions at $z = 7.5$, 11.9, 16.1, and 21.0 Å. After the transition state at $z = 20.4$ Å (see Fig. 6(a)), the system transiently passes through the two+two-ion state (S_{2+2}) when the ion transport is taking place. The positions of ions ($z = 6.4$, 10.9, 15.3, and 19.8 Å) in this temporal S_{2+2} state are indicated with the green arrows in Fig. 6; two ions are inside of ANT and two ions are locating in the vicinity of the entrance and the exit. The energy profile has the maxima at S_{2+2} due to the peaks of $E_{\text{ion-water}} + E_{\text{ion-ANT}}$ when the incoming ions are dehydrated and then the outgoing ions are rehydrated after a while.

Then the ions find small energy dips at $z = 5.0$, 9.9, 14.1, and 18.6 Å (Fig. 6(b)), noted as S_{1+3}, where the left most ion is already outside of $ANT^{-6.0}$. The S_{1+3} state corresponds to the maximum of the two-dimensional free energy surface shown in Fig. 6(a), where the ion-ion repulsion, $E_{\text{ion-ion}}$, has its maximum. The transition path sampling analysis shows that the S_{1+3} state has more than 95% probability of the ion permeation, thus S_{1+3} is not a true transition state.[72] The left most ion immediately leaves to the bulk due to the strong ion-ion repulsion. The overall process of the ion permeation in $ANT^{-6.0}$ can, therefore, be written as $S_3 \rightarrow S_{3+1} \rightarrow S_{2+2} \rightarrow S_{1+3} \rightarrow S_3$. The steps of $S_{2+2} \rightarrow S_{1+3} \rightarrow S_3$, where the fourth ion entering to ANT pushes out one ion from the other end (exit) of ANT via pushing two ions in between,[74–76] are very fast. This part of the ion transport process may look like the so-called knock-on type permeation. There exists, however, the rate-determining step between $S_{3+1} \rightarrow S_{2+2}$ even in $ANT^{-6.0}$ as described above.

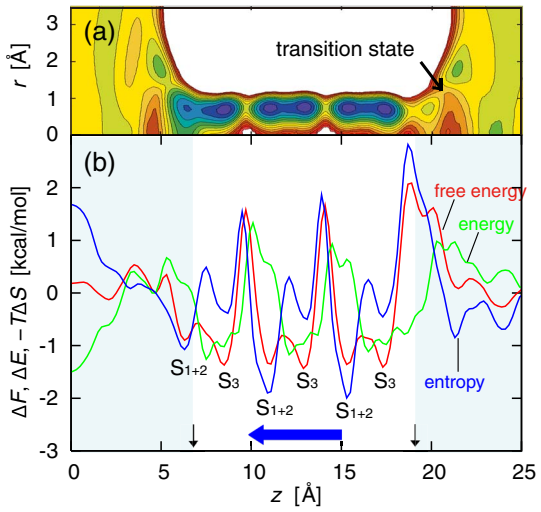

FIG. 7. Free energy (ΔF), energy (ΔE), and entropy ($-T\Delta S$) profiles for ion permeation through ANT$^{-5.4}$. The length of ANT is 12 Å. (a) The two-dimensional plot of the free energy along z and r. The method of coloring is the same as in Fig. 1(a). (b) Free energy, energy, and entropy along z are indicated in red, green, and blue lines, respectively. The meaning of arrows and coloring are the same as in Fig. 1(b). The entropy barrier at the entrance is lower by 0.6 kcal/mol than that in ANT$^{-5.0}$. On the other hand, the energy profile is similar to that in ANT$^{-5.0}$, so there is no large energy barrier seen in ANT$^{-6.0}$. Thus, the balance of the energy and entropy contributes to the most efficient ion permeation in ANT$^{-5.4}$. The overall process of the ion permeation is expressed as $S_3 \rightarrow S_{1+2} \rightarrow S_3$.

V. MECHANISM OF ION PERMEATION THROUGH ANT WITH CHARGE OF −5.4E

Figure 7(b) plots the free energy, energy, and entropy ($-T\Delta S$) profiles for ion permeation through ANT$^{-5.4}$. Their characters are the mixtures of those for ANT$^{-5.0}$ and for ANT$^{-6.0}$, since there are two modes of ion permeation through ANT$^{-5.4}$: one is the process that the third ion enters into ANT$^{-5.4}$ containing two ions like ANT$^{-5.0}$, the other is that the fourth ion enters into ANT$^{-5.4}$ containing three ions like ANT$^{-6.0}$.[59] The energy profile is less rugged than that in ANT$^{-6.0}$. The strong ion-ion repulsion seen in ANT$^{-6.0}$ is suppressed in ANT$^{-5.4}$, because the distance between ions is larger than that in ANT$^{-6.0}$.

We can see in the figure that the free energy profiles consist of two sets of minima. The first set contains minima at $z = 8.5$, 13.0, and 17.3 Å (S_3), while the second one at $z = 6.3$, 11.1, and 15.3 Å (S_{1+2}). The free energies of these two states, connected with a very low free energy barrier, are almost the same. The ions indeed fluctuate between these two conformations in MD simulations.[59] Figure 7 shows that S_3 is stabilized by the energy contribution, while S_{1+2} is mostly by the entropy ($-T\Delta S$). The efficient ion permeation is observed in ANT$^{-5.4}$ where the energy and entropic contributions are well balanced.[59]

VI. MECHANISM OF ION PERMEATION THROUGH ANT WITH DIFFERENT LENGTHS

We have performed 12 simulations as the combination of the length (8, 10, 12, and 14 Å) and the charge on ANT (−5.0, −5.4, and −6.0e) to examine the effects of the length and charge of ANT. The rates of the ion permeation obtained are listed in Table I. The lower subscript indicates the length of ANT hereafter (Figs. 1–4 are for ANT$_{12}^{-5.0}$).

The entropy barrier at the entrance arisen from the ion-WAT2 exchange is low through short ANTs such as ANTs with a length of 8 or 10 Å, since WAT2 in them is exposed to the bulk as that in ANT$_{12}^{-6.0}$. On the other hand, an entropy barrier is evident through ANTs with a length of 14 Å, because the ion-WAT2 exchange must take place inside ANT, as in ANT$_{12}^{-5.0}$ case.

The energy barriers in ANT$_{10}^{-5.0}$, ANT$_{10}^{-5.4}$, and ANT$_{10}^{-6.0}$ are not large, because they hold two ions and thus the ion-ion repulsion is not large. Hence, the free energy barriers are low and the ion conductance is high. Since the number of atoms in ANTs with a length of 8 Å is smaller than that in longer ANTs, the charges on the anion atoms of these ANTs are larger (Table I), which makes the ion-ANT interaction larger. Accordingly, the dissociation of an ion from the ANT exit to the bulk is difficult, leading to low conductance. ANT$_{14}^{-5.0}$ and ANT$_{14}^{-5.4}$ constantly contain three ions, and thus the large energy barrier for ion permeation emerges due to the strong ion-ion repulsion when the ion permeation occurs. Thus, the rate of ion permeation is small in these ANTs. In ANT$_{14}^{-6.0}$, the S_{3+1} state is metastable because of the lengthened ion-ion distance, thus ion permeation is faster than ANT$_{14}^{-5.0}$ and ANT$_{14}^{-5.4}$.

The rate of the ion permeation of ANT$_{10}^{-6.0}$ is about 80 times faster than that through ANT$_{14}^{-5.0}$. It means that a slight modification of the charge and the length causes a significant change of the permeability of an ion transporter.

The ratio of the number of ions which enter ANT$_{10}^{-6.0}$ over that of ions which approach the entrance is 39%. This ratio is the highest in all the ANTs used in this study and is four times larger than that in ANT with a length of 12 Å.[59] This

TABLE I. Rates of ion permeation through various ANTs. The rates are defined as the number of ion permeation events in 1 ns. The standard deviations were estimated by block averaging. The number in parenthesis shows the number of ions in ANT. Second row indicates the partial charge on each anion atom of ANT.

Length of ANT	8 Å	10 Å	12 Å	14 Å
ANT$^{-5.0}$	0.56 ± 0.12 (2)	1.96 ± 0.33 (2)	0.34 ± 0.03 (2)	0.04 ± 0.05 (3)
	−0.625e	−0.500e	−0.417e	−0.357e
ANT$^{-5.4}$	0.45 ± 0.13 (2)	2.48 ± 0.38 (2)	0.56 ± 0.03 (2/3)	0.16 ± 0.08 (3)
	−0.675e	−0.540e	−0.450e	−0.386e
ANT$^{-6.0}$	0.52 ± 0.10 (2)	3.44 ± 0.42 (2)	0.36 ± 0.06 (3)	0.50 ± 0.11 (3)
	−0.750e	−0.600e	−0.500e	−0.429e

means the permeation mechanism becomes close to the so-called knock-on type,[74,75] however, it is notable that 61% of ions which approach the entrance still go back to the bulk.

VII. CONCLUSIONS

The mechanism of ion permeation through the model channel, ANT, was investigated by analyzing the energy and entropic contributions to the free energy profile. It was found that the dynamics of the ion permeation through ANT is governed by the subtle balance between the energy and entropic contributions. The interplay of these two contributions, when well balanced, causes the smooth number alternation of ions inside ANT as $3 \rightarrow 2 \rightarrow 3 \rightarrow 2$ and so on, "automating" the ion permeation process. The dominant free energy barrier existing at the entrance of ANT is caused by the entropy bottleneck, namely, due to the narrow phase space for the entering ion-WAT2 exchange. This indicates that the transport of water molecules in CNT or in the aquaporin must be fast, since such coordination exchange between ion and water molecule does not exist there.[15,77]

In $ANT^{-5.0}$, the permeation is thoroughly the entropy bottleneck at the entrance. In contrast, the energy term as well as the entropy term are responsible for the ion permeation rate through $ANT^{-6.0}$. It is notable that ion-ion repulsion seen in $ANT^{-6.0}$ does not necessarily facilitate the permeation. In $ANT^{-5.4}$, these two terms are balanced, resulting in the highest ion conductance in these three cases.

It was shown that the balance between the energy and entropic contributions, which can be controlled by changing the length and charge of ANT, determines the rate of the permeation. A part of ion permeation processes through ANT with the larger negative charge, −6.0e, shows the so-called knock-on type behavior,[74–76] and the ions inside ANT are pushed by the energetic repulsion of an incoming ion. It is, however, not of the simple Newton's ball type because most of ions approaching the ANT entrance are repelled away. It is noteworthy that this knock-on type transport is not necessarily the fastest ion permeation process. When the length and charge are suitably selected, the much more efficient ion permeation is obtained, since the ion conduction is governed by the interplay of the energy and entropic contributions.

In the real ion channel system, the saturation of the current-voltage curves at the high voltage has historically been considered to be the evidence that the ion permeation is controlled by the ion diffusion unrelated to the electric field or the energy term.[78] Our previous work, however, demonstrated that the ion permeation through ANT is not diffusion limited.[59] In addition, we revealed here the ion conduction is limited by the entropy term originated from the ion-WAT2 exchange. These two studies suggest a new interpretation for the ion conduction mechanism: the saturation can be a sign of the entropy bottleneck.

It was seen that the ion permeation is very sensitive to how the incoming ion is coordinated to WAT1 by exchanging the positions of ion-WAT2. Such ion-WAT exchange mechanism, which is a part of the ion dehydration, must be sensitive to the ion species. The nanopores with wider diameters are expected to be poor ion selectors because the exchange of the entering ion and WAT2 is not required to take place. Further investigation is needed to study how the balance between the energy and entropic contributions changes for the different ion species in order to understand the ion selectivity.[43,49,79,80] The electronic effects such as the polarization were reported to be important in the ion translocation process in some biological channels.[18,71,81,82] It should be also investigated how the polarization effects change the height of the free energy barrier, though it is expected that the entropy barrier at the entrance arisen from the exchange process would be still present, since the exchange must exist regardless of the potential parameter used.

ACKNOWLEDGMENTS

T.S. is grateful to Professor S. Oiki and Dr. H. Shimizu, Dr. M. Iwamoto, and Dr. M. Kamiya for valuable discussion. The present study was supported by the Grant-in Aid for Scientific Research (No. 25288011). The calculation has been carried out by using the supercomputers at Research Center for Computational Science in Okazaki.

[1] A. I. Skoulidas, D. M. Ackerman, J. K. Johnson, and D. S. Sholl, Phys. Rev. Lett. **89**, 185901 (2002).
[2] M. Majumder, N. Chopra, R. Andrews, and B. J. Hinds, Nature (London) **438**, 44 (2005).
[3] J. K. Holt, H. G. Park, Y. Wang, M. Stadermann, A. B. Artyukhin, C. P. Grigoropoulos, A. Noy, and O. Bakajin, Science **312**, 1034 (2006).
[4] S. R. Majumder, T. Bandyopadhyay, and S. K. Ghosh, J. Chem. Phys. **125**, 201103 (2006).
[5] K. B. Jirage, J. C. Hulteen, and C. R. Martin, Science **278**, 655 (1997).
[6] J. H. Park, S. B. Sinnott, and N. R. Aluru, Nanotechnology **17**, 895 (2006).
[7] M. Majumder, X. Zhan, R. Andrews, and B. J. Hinds, Langmuir **23**, 8624 (2007).
[8] S. Kim, L. Chen, J. K. Johnson, and E. Marand, J. Membr. Sci. **294**, 147 (2007).
[9] H. B. Park, C. H. Jung, Y. M. Lee, A. J. Hill, S. J. Pas, S. T. Mudie, E. V. Wagner, B. D. Freeman, and D. J. Cookson, Science **318**, 254 (2007).
[10] L. Liu and X. Chen, J. Phys. Chem. B **113**, 6473 (2009).
[11] Y. Xie, Y. Kong, A. K. Soh, and H. Gao, J. Chem. Phys. **127**, 225101 (2007).
[12] U. Zimmerli and P. Koumoutsakos, Biophys. J. **94**, 2546 (2008).
[13] V. V. Chaban, T. I. Savchenko, S. M. Kovalenko, and O. V. Prezhdo, J. Phys. Chem. B **114**, 13481 (2010).
[14] C. Wei and D. Srivastava, Phys. Rev. Lett. **91**, 235901 (2003).
[15] G. Hummer, J. C. Rasaiah, and J. P. Noworyta, Nature (London) **414**, 188 (2001).
[16] C. Peter and G. Hummer, Biophys. J. **89**, 2222 (2005).
[17] H. Liu, S. Murad, and C. J. Jameson, J. Chem. Phys. **125**, 084713 (2006).
[18] D. Lu, Y. Li, U. Ravaioli, and K. Schulten, Phys. Rev. Lett. **95**, 246801 (2005).
[19] L. Yang and S. Garde, J. Chem. Phys. **126**, 084706 (2007).
[20] B. Corry, J. Phys. Chem. B **112**, 1427 (2008).
[21] C. Song and B. Corry, J. Phys. Chem. B **113**, 7642 (2009).
[22] H. Lu, X. Zhou, F. Wu, and Y. Xu, J. Phys. Chem. B **112**, 16777 (2008).
[23] X. Gong, J. Li, K. Xu, J. Wang, and H. Yang, J. Am. Chem. Soc. **132**, 1873 (2010).
[24] M. Yu, H. H. Funke, J. L. Falconer, and R. D. Noble, J. Am. Chem. Soc. **132**, 8285 (2010).
[25] T. A. Beu, J. Chem. Phys. **132**, 164513 (2010).
[26] T. A. Hilder, D. Gordon, and S.-H. Chung, Biophys. J. **99**, 1734 (2010).
[27] J. J. Cannon, D. Tang, N. Hur, and D. Kim, J. Phys. Chem. B **114**, 12252 (2010).
[28] Q. Shao, L. Huang, J. Zhou, L. Lu, L. Zhang, X. Lu, S. Jiang, K. E. Gubbins, and W. Shen, Phys. Chem. Chem. Phys. **10**, 1896 (2008).
[29] A. Izadi-Najafabadi, D. N. Futaba, S. Iijima, and K. Hata, J. Am. Chem. Soc. **132**, 18017 (2010).

[30]C. Dellago, M. M. Naor, and G. Hummer, Phys. Rev. Lett. **90**, 105902 (2003).
[31]D. J. Mann and M. D. Halls, Phys. Rev. Lett. **90**, 195503 (2003).
[32]Z. Cao, Y. Peng, T. Yan, S. Li, A. Li, and G. A. Voth, J. Am. Chem. Soc. **132**, 11395 (2010).
[33]A. Waghe, J. C. Rasaiah, and G. Hummer, J. Chem. Phys. **137**, 044709 (2012).
[34]G. M. Preston, T. P. Carroll, W. B. Guggino, and P. Agre, Science **256**, 385 (1992).
[35]D. A. Doyle, J. M. Cabral, R. A. Pfuetzner, A. Kuo, J. M. Gulbis, S. L. Cohen, B. T. Chait, and R. MacKinnon, Science **280**, 69 (1998).
[36]B. L. de Groot and H. Grumbmüller, Science **294**, 2353 (2001).
[37]E. Tajkhorshid, P. Nollert, M. Ø. Jensen, L. J. W. Miercke, J. O'Connell, R. M. Stroud, and K. Schulten, Science **296**, 525 (2002).
[38]N. Chakrabarti, B. Roux, and R. Pomès, J. Mol. Biol. **343**, 493 (2004).
[39]J. Åqvist and V. Luzhkov, Nature (London) **404**, 881 (2000).
[40]L. Guidoni, V. Torre, and P. Carloni, FEBS Lett. **477**, 37 (2000).
[41]S. Bernèche and B. Roux, Nature (London) **414**, 73 (2001).
[42]S. Bernèche and B. Roux, Proc. Natl. Acad. Sci. U.S.A. **100**, 8644 (2003).
[43]S. Y. Noskov, S. Bernèche, and B. Roux, Nature (London) **431**, 830 (2004).
[44]F. Khalili-Araghi, E. Tajkhorshid, and K. Schulten, Biophys. J. **91**, L72 (2006).
[45]C. Domene, S. Vemparala, S. Furini, K. Sharp, and M. L. Klein, J. Am. Chem. Soc. **130**, 3389 (2008).
[46]S. Furini and C. Domene, Proc. Natl. Acad. Sci. U.S.A. **106**, 16074 (2009).
[47]M. Ø. Jensen, D. W. Borhani, K. Lindorff-Larsen, P. Maragakis, V. Jogini, M. P. Eastwood, R. O. Dror, and D. E. Shaw, Proc. Natl. Acad. Sci. U.S.A. **107**, 5833 (2010).
[48]W. Treptow and M. L. Klein, J. Am. Chem. Soc. **132**, 8145 (2010).
[49]B. Egwolf and B. Roux, J. Mol. Biol. **401**, 831 (2010).
[50]L. Delemotte, M. Tarek, M. L. Klein, C. Amaral, and W. Treptow, Proc. Natl. Acad. Sci. U.S.A. **108**, 6109 (2011).
[51]M. Ø. Jensen, V. Jogini, M. P. Eastwood, and D. E. Shaw, J. Gen. Physiol. **141**, 619 (2013).
[52]P. S. Crozier, R. L. Rowley, N. B. Holladay, D. Henderson, and D. D. Busath, Phys. Rev. Lett. **86**, 2467 (2001).
[53]M. L. Brewer, U. W. Schmitt, and G. A. Voth, Biophys. J. **80**, 1691 (2001).
[54]O. Beckstein and M. S. P. Sansom, Proc. Natl. Acad. Sci. U.S.A. **100**, 7063 (2003).
[55]J. Dzubiella, R. J. Allen, and J. P. Hansen, J. Chem. Phys. **120**, 5001 (2004).
[56]S. Joseph, R. J. Mashl, E. Jakobsson, and N. R. Aluru, Nano Lett. **3**, 1399 (2003).
[57]F. Zhu and K. Schulten, Biophys. J. **85**, 236 (2003).
[58]C. F. Lopez, S. O. Nielsen, P. B. Moore, and M. L. Klein, Proc. Natl. Acad. Sci. U.S.A. **101**, 4431 (2004).
[59]T. Sumikama, S. Saito, and I. Ohmine, J. Phys. Chem. B **110**, 20671 (2006).
[60]W. L. Jorgensen, J. Chandrasekhar, J. D. Madura, R. W. Impey, and M. L. Klein, J. Chem. Phys. **79**, 926 (1983).
[61]W. D. Cornell, P. Cieplak, C. I. Bayly, I. R. Gould, K. M. Merz, Jr., D. M. Ferguson, D. C. Spellmeyer, T. Fox, J. W. Caldwell, and P. A. Kollman, J. Am. Chem. Soc. **117**, 5179 (1995).
[62]H. J. C. Berendsen, J. P. M. Postma, W. F. van Gunsteren, A. DiNola, and J. R. Haak, J. Chem. Phys. **81**, 3684 (1984).
[63]J. P. Ryckaert, G. Ciccotti, and H. J. C. Berendsen, J. Comput. Phys. **23**, 327 (1977).
[64]U. Essmann, L. Parera, M. L. Berkowitz, T. Darden, H. Lee, and J. G. Pedersen, J. Chem. Phys. **103**, 8577 (1995).
[65]L. Delemotte, M. L. Klein, and M. Tarek, Front. Pharmacol. **3**, 97 (2012).
[66]O. S. Andersen, Biophys. J. **41**, 147 (1983).
[67]A. K. Ballard and C. Dellago, J. Phys. Chem. B **116**, 13490 (2012).
[68]M. Ø. Jensen, S. Park, E. Tajkhorshid, and K. Schulten, Proc. Natl. Acad. Sci. U.S.A. **99**, 6731 (2002).
[69]See supplementary material at http://dx.doi.org/10.1063/1.4827088 for movies S1 and S2.
[70]G. Portella, J. S. Hub, M. D. Vesper, and B. L. de Groot, Biophys. J. **95**, 2275 (2008).
[71]T. W. Allen, O. S. Andersen, and B. Roux, Proc. Natl. Acad. Sci. U.S.A. **101**, 117 (2004).
[72]P. G. Bolhuis, D. Chandler, C. Dellago, and P. L. Geissler, Annu. Rev. Phys. Chem. **53**, 291 (2002).
[73]R. Kubo, M. Toda, and N. Hashitsume, *Statistical Physics II: Nonequilibrium Statistical Mechanics* (Springer-Verlag, New York, 1992), p. 61.
[74]A. L. Hodgkin and R. D. Keynes, J. Physiol. **128**, 61 (1955).
[75]C. Miller, Nature (London) **414**, 23 (2001).
[76]P. H. A. Nelson, J. Chem. Phys. **134**, 165102 (2011).
[77]M. L. Zeidel, S. V. Ambudkar, B. L. Smith, and P. Agre, Biochemistry **31**, 7436 (1992).
[78]O. S. Andersen, R. E. Koeppe II, and B. Roux, IEEE Trans. Nanobiosci. **4**, 10 (2005).
[79]H. Yu and B. Roux, Biophys. J. **97**, L15 (2009).
[80]B. Corry and M. Thomas, J. Am. Chem. Soc. **134**, 1840 (2012).
[81]S. Patel, J. E. Davis, and B. A. Bauer, J. Am. Chem. Soc. **131**, 13890 (2009).
[82]D. Bucher and S. Kuyucak, Chem. Phys. Lett. **477**, 207 (2009).